Pergamon
www.elsevier.com/locate/jappmathmech
PII: S0021-8928(03)00069-8
J. Appl. Maths Mechs, Vol. 67, No. 3, pp. 407–416, 2003

0021-8928/$—see front matter

THE ACTION OF AN UNSTEADY EXTERNAL LOAD ON A CIRCULAR ELASTIC PLATE FLOATING ON SHALLOW WATER†

I. V. STUROVA

Novosibirsk

(*Received* 25 *March* 2002)

A solution of the transient problem of the behaviour of a circular elastic plate floating on the free surface of a liquid under the action of an external load is constructed. It is assumed that the liquid is ideal and incompressible and that its depth is small compared with the radius of the plate. The compatible motion of the plate and the liquid is treated within the framework of linear theory. The flow of the liquid is assumed to be irrotational. The behaviour of the plate under different loads is investigated and it is shown that the bounded dimensions of the elastic plate have a substantial effect on its unsteady behaviour. © 2003 Elsevier Ltd. All rights reserved.

The action of periodic surface pressures on a circular platform floating on the surface of a liquid of finite depth has been investigated earlier [1]. In the planar case, girders of finite and semi-infinite length were considered and, in the spatial case, a circular plate. The oscillations of the liquid and the plate were assumed to be steady. This problem is a special case of the transient problem of the action of an external dynamic load on a floating elastic plate. The unsteady behaviour of an elastic plate which is unbounded in plan has been studied quite thoroughly (sec [2–4], for example) as applied to the investigation of the effect of a moving external load on an ice sheet. Examples of calculations have been presented for a rectangular plate [5, 6]. The planar problem of the unsteady behaviour of an elastic beam of finite length floating on shallow water has been investigated [7] in the case of different external loads, with an without allowing for the inertia of the load.

1. FORMULATION OF THE PROBLEM

Suppose a homogeneous circular elastic plate of radius r_0 floats in the surface layer of an ideal incompressible liquid of depth H. The surface of the liquid not covered by the plate is free. The liquid flow is assumed to be irrotational. We will denote the velocity potentials of the liquid in the domain under the plate and outside this domain by $\phi^{(1)}(x, y, t)$ and $\phi^{(2)}(x, y, t)$ respectively, where x and y are the horizontal coordinates with the origin of coordinates at the centre of the plate.

The normal deflection of an elastic plate $w(x, y, t)$ is described by the equation (a time derivative is denoted by a dot)

$$D\Delta^2 w + \rho_1 h_1 \ddot{w} + g\rho w + \rho\dot{\phi}^{(1)} = -P(x, y, t), \quad r \le r_0 \tag{1.1}$$

where

$$\Delta = \partial^2/\partial x^2 + \partial^2/\partial y^2, \quad r = \sqrt{x^2 + y^2}, \quad D = Eh_1^3/[12(1-\nu^2)]$$

E, ρ_1, h_1 ν are the modulus of normal elasticity, the density, the thickness and Poisson's ratio of the plate, ρ is the density of water and g is the acceleration due to gravity. The function $P(x, y, t)$ is specified and describes the external pressure acting on the plate.

According to linear shallow-water theory, the following relation holds

$$\dot{w} = -h\Delta\phi^{(1)}, \quad r \le r_0; \quad h = H - d \tag{1.2}$$

where $d = \rho_1 h_1/\rho$ is the setting of the plate.

†*Prikl. Mat. Mekh.* Vol. 67, No. 3, pp. 453–463, 2003.

In the clear water region, the velocity potential $\phi^{(1)}(x, y, t)$ satisfies the equation

$$\ddot{\phi}^{(2)} = gH\Delta\phi^{(2)} \quad (r > r_0) \tag{1.3}$$

with the attenuation condition $\phi^{(2)} \to 0$ $(r \to \infty)$.

The assumption that the liquid, when $r > r_0$, is weightless is used in collision theory when investigating short-term external action on a floating elastic plate [8] and then, instead of Eq. (1.3), we have

$$\phi^{(2)}(x, y, t) = 0, \quad r > r_0 \tag{1.4}$$

When $r = r_0$, the following conditions of continuity of the pressure and mass flow must be satisfied

$$\dot{\phi}^{(1)} = \dot{\phi}^{(2)}, \quad \partial\phi^{(1)}/\partial r = (H/h)\partial\phi^{(2)}/\partial r \tag{1.5}$$

The conditions of a free edge, that is, that the bending moment and the shearing force are zero, are imposed on the edges of the plate

$$\Delta w - \frac{\nu_1}{r}\left(\frac{1}{r}\frac{\partial^2 w}{\partial\theta^2} + \frac{\partial w}{\partial r}\right) = \frac{\partial\Delta w}{\partial r} + \frac{\nu_1}{r^2}\frac{\partial^2}{\partial\theta^2}\left(\frac{\partial w}{\partial r} - \frac{w}{r}\right) = 0, \quad r = r_0$$

where

$$\theta = \operatorname{arctg}(y/x), \quad \nu_1 = 1 - \nu$$

We will assume that, at the initial instant of time, the liquid and the plate are at rest. Then,

$$w = \dot{w} = \phi^{(1)} = \phi^{(2)} = \dot{\phi}^{(2)} = 0, \quad t = 0 \tag{1.6}$$

Next, we change to the dimensionless variables (denoted by primes)

$$(x', y', H', h') = \frac{(x, y, H, h)}{r_0}, \quad t' = \sqrt{\frac{g}{r_0}}t, \quad w' = \frac{w}{a}, \quad \phi'_{1,2} = \frac{\phi_{1,2}}{a\sqrt{gr_0}}, \quad P' = \frac{P}{a\rho g}$$

where a is a factor having the dimension of length. The following dimensionless coefficients will be used below

$$\beta = \frac{H}{h}, \quad \gamma = \frac{d}{r_0}, \quad \delta = \frac{D}{\rho g r_0^4}$$

2. EXPANSION IN NATURAL OSCILLATIONS

For simplicity, we will assume that the external pressure in Eq. (1.1) is an even function of y and, consequently, the deflections of the plate are symmetrical about the x axis. In the dimensionless variables (the primes are henceforth omitted), we shall seek the deflection of the plate in the form of an expansion in the natural oscillations of a circular plate with free edges in a vacuum

$$w(r, \theta, t) = \sum_{n=0}^{\infty} \cos n\theta \sum_{j=0}^{\infty} a_{jn}(t) W_{jn}(r) \tag{2.1}$$

where $a_{jn}(t)$ are unknown functions of time, to be determined, and $W_{jn}(r)$ is the solution of the eigenvalue problem

$$L_n W_{jn} = \lambda_{jn}^4 W_{jn}, \quad r \le 1; \quad L_n = \frac{d^2}{dr^2} + \frac{1}{r}\frac{d}{dr} - \frac{n^2}{r^2}$$

$$W''_{jm} + \nu W'_{jn} - n^2\nu W_{jn} = (L_n W_{jn})' + n^2\nu_1(W_{jn} - W'_{jn}) = 0, \quad r = 1$$

where a prime denotes differentiation with respect to r. This eigenvalue problem has been studied in detail in [9, 10]. All the eigenfunctions, apart from $W_{00} = \sqrt{2}$ and $W_{01} = 2r$, which are modes of motion of a rigid body and correspond to the characteristic numbers $\lambda_{00} = \lambda_{01} = 0$, have the form

$$W_{jn} = A_{jn}[J_n(\lambda_{jn}r) + C_{jn}I_n(\lambda_{jn}r)]$$

where

$$C_{jn} = \frac{\lambda_{jn}^2 J_n(\lambda_{jn}) + \nu_1[\lambda_{jn}J_n'(\lambda_{jn}) - n^2 J_n(\lambda_{jn})]}{\lambda_{jn}^2 I_n(\lambda_{jn}) - \nu_1[\lambda_{jn}I_n'(\lambda_{jn}) - n^2 I_n(\lambda_{jn})]} =$$

$$= \frac{\lambda_{jn}^3 J_n'(\lambda_{jn}) + n^2\nu_1[\lambda_{jn}J_n'(\lambda_{jn}) - J_n(\lambda_{jn})]}{\lambda_{jn}^3 I_n'(\lambda_{jn}) - n^2\nu_1[\lambda_{jn}I_n'(\lambda_{jn}) - I_n(\lambda_{jn})]}$$

$$A_{j0}^{-2} = \frac{1}{2}\left\{J_0^2(\lambda_{j0}) + J_1^2(\lambda_{j0}) + \frac{2C_{j0}}{\lambda_{j0}}[I_1(\lambda_{j0})J_0(\lambda_{j0}) + I_0(\lambda_{j0})J_1(\lambda_{j0})] + \right.$$

$$\left. + C_{j0}^2[I_0^2(\lambda_{j0}) - I_1^2(\lambda_{j0})]\right\}, \quad j \geq 1 \tag{2.2}$$

$$A_{jn}^{-2} = \frac{1}{2}\left\{J_n^2(\lambda_{jn}) - J_{n-1}(\lambda_{jn})J_{n+1}(\lambda_{jn}) + \frac{2C_{jn}}{\lambda_{jn}}[I_{n+1}(\lambda_{jn})J_n(\lambda_{jn}) + I_n(\lambda_{jn})J_{n+1}(\lambda_{jn})] + \right.$$

$$\left. + C_{jn}^2[I_n^2(\lambda_{jn}) - I_{n-1}(\lambda_{jn})I_{n+1}(\lambda_{jn})]\right\}, \quad j, n \geq 1$$

J_n and I_n are normal and modified Bessel functions of the first kind. The characteristic numbers λ_{jn} ($\lambda_{jn} > \lambda_{j+1n}$) are determined from the dispersion relation, which follows form (2.2). The set of functions W_{jn} forms a complete orthogonal system with the normalization condition

$$\int_0^1 rW_{jn}(r)W_{kn}(r)dr = \delta_{jk}$$

where δ_{jk} is the Kronecker delta. Numerical values of λ_{jn}, C_{jn} and A_{jn} are given in [10] for the first 701 modes when $\nu = 0.33$.

Using the condition of symmetry with respect to the angular coordinate θ, we represent the potentials $\phi^{(1,2)}(r, \theta, t)$ in the form

$$\phi^{(1,2)}(r, \theta, t) = \sum_{n=0}^{\infty} \Phi_n^{(1,2)}(r, t)\cos n\theta \tag{2.3}$$

Using expansions (2.1) and (2.3), we seek a solution for $\Phi_n^{(1)}(r, t)$, which satisfies Eq. (1.2), in the form

$$\Phi_n^{(1)}(r, t) = -\frac{1}{h}\left\{\sum_{j=0}^{\infty} \dot{a}_{jn}(t)[\Psi_{jn}(r) - r^n\Psi_{jn}(1)] + r^n q_n(t)\right\} \tag{2.4}$$

The functions $\Psi_{jn}(r)$ are determined from the equation

$$L_n\Psi_{jn}(r) = W_{jn}(r)$$

For the rigid-body modes

$$\Psi_{00}(r) = \frac{r^2}{2\sqrt{2}}, \quad \Psi_{01}(r) = \frac{r^3}{4}$$

and for the remaining modes

$$\Psi_{jn} = \frac{A_{jn}}{\lambda_{jn}^2}[C_{jn}I_n(\lambda_{jn}r) - J_n(\lambda_{jn}r)]$$

The functions $q_n(t)$ and expression (2.4) are unknown. Assuming the liquid to be weightless when $r > 1$, according to Eq. (1.4) we have $q_n \equiv 0$ and, in the case of a ponderable liquid, these functions are determined from the matching conditions for the potentials $\Phi_n^{(1)}(r, t)$, $\Phi_n^{(2)}(r, t)$ along the perimeter of the plate and their derivatives with respect to r

$$\Phi_n^{(1)} = \Phi_n^{(2)}, \quad \partial\Phi_n^{(1)}/\partial r = \beta\partial\Phi_n^{(2)}/\partial r, \quad r = 1$$

which follow from relations (1.5).

According to Eq. (1.3), the equation for $\Phi_n^{(2)}(r, t)$ has the form

$$\ddot{\Phi}_n^{(2)} = HL_n\Phi_n^{(2)}, \quad r > 1; \quad \Phi_n^{(2)} \to 0, \quad r \to \infty$$

The properties of the solutions of this equation were described in detail in [11] when investigating the problem of the diffraction of acoustic waves by a rigid circular cylinder.

We introduce the notation

$$\Phi_n^{(2)}\big|_{r=1} = S_n(t), \quad \partial\Phi_n^{(2)}/\partial r\big|_{r=1} = T_n(t)$$

Applying a Laplace integral transformation, we obtain the following relations which connect these functions.

$$S_n(t) = \sqrt{H}\int_0^t T_n(\tau)G_n(\sqrt{H}(t-\tau))d\tau \tag{2.5}$$

where the so-called transition function has the form

$$G_n(\xi) = \frac{1}{2i\pi}\int_{\sigma-i\infty}^{\sigma+i\infty}\frac{K_n(s)}{sK_n'(s)}\exp(s\xi)ds \tag{2.6}$$

Here, K_n are modified Bessel functions of the second kind and the quantity σ is chosen such that the path of integration on the right-hand side of equality (2.6) lies to the right of all the singular points of the integrand. The transition functions $G_n(\xi)$ have been tabulated in [12] for up to $n = 10$, simple approximations of them have been proposed in [13] and a graphical comparison of the exact and approximate solution has also been given in [13].

We now substitute expansions (2.1), (2.3) and (2.4) into the dimensionless analogue of Eq. (1.1) and the initial conditions (1.6), multiply the resulting relations by $r\cos(n\theta)W_{kn}(r)$ and integrate them with respect to r within the limits from 0 to 1 and with respect to θ within the limits from 0 to 2π. Using the properties of the functions $W_{kn}(r)$, we obtain the following system of ordinary differential equations (ODE)

$$\sum_{j=0}^{\infty}\ddot{a}_{jn}\left[\gamma\delta_{kj} - \frac{1}{h}D_{kj}^{(n)}\right] + (1 + \delta\lambda_{kj}^4)a_{kn} - \frac{1}{h}S_{kn}\dot{q}_n = -P_{kn} \quad (k = 0, 1, 2\ldots) \tag{2.7}$$

(a dot now denotes a total derivative with respect to time) with the boundary conditions

$$a_{kn}(0) = \dot{a}_{kn}(0) = q_n(0) = 0$$

Here,

$$D_{kj}^{(n)} = \int_0^1 rW_{kn}(r)[\Psi_{jn}(r) - r^n\Psi_{jn}(1)]dr, \quad D_{kj}^{(n)} = D_{jk}^{(n)} \tag{2.8}$$

$$S_{kn} = \int_0^1 r^{n+1} W_{kn}(r)dr \tag{2.9}$$

$$P_{kn}(t) = \frac{\varepsilon_n}{\pi}\int_0^{\pi}\cos(n\theta)d\theta\int_0^1 rP(r,\theta,t)W_{kn}(r)dr, \quad \varepsilon_0 = 1, \quad \varepsilon_n = 2 \quad (n \geq 1) \tag{2.10}$$

The integrodifferential equation, which is a consequence of relation (2.5).

$$q_n(t) = \frac{h}{\sqrt{H}}\int_0^t\left[\sum_{j=0}^{\infty}\dot{a}_{jn}(\tau)b_{jn} + nq_n(\tau)\right]G_n(\sqrt{H}(t-\tau))d\tau \tag{2.11}$$

where

$$b_{jn} = \partial\Psi_{jn}/\partial r|_{r=1} - n\Psi_{jn}(1)$$

closes this system of ordinary differential equations.

It can be shown that $S_{kn} = b_{kn}$. The system of integrodifferential equations (2.7), (2.11) is somewhat simplified with $n = 0, 1$ when all of the values of S_{kn} are equal to zero apart from $S_{00} = 1/\sqrt{2}$ and $S_{01} = 1/2$.

3. METHOD OF NUMERICAL SOLUTION

Using the reduction method, the infinite series in relations (2.1), (2.3) and (2.4) are replaced by finite sums with a number of terms N in the expansion in angular harmonics and taking account of the first M eigenfunctions. The integration in (2.8) and (2.9) is carried out analytically while, in (2.1) in the case of an arbitrary distribution of the external pressure $P(r, \theta, t)$, the double integral is evaluated numerically.

The equations (2.7) and (2.11) are solved by the method of finite differences with a constant time step. The method described earlier in [6] is used to calculate the convolution-type integral in (2.11).

We will now briefly describe it by taking the evaluation of the integral

$$F(t) = \int_0^t V(\tau)Z(t-\tau)d\tau \tag{3.1}$$

as the example.

For an instant of time $t = K\zeta$, where ζ is the time step, integral (3.1) can be written in the form

$$F(K\zeta) = \sum_{n=0}^{K-1}\int_{t_k}^{t_{k+1}} V(\tau)Z(t-\tau)d\tau, \quad t_k = k\zeta \tag{3.2}$$

We denote the values of the functions $V(t)$ and $Z(t)$ at the instants of time t_k by V_k and $z_k (k = 0, 1, 2, \ldots, K)$ respectively. It is assumed that, when $k < K$, these values are known. When $t_k \leq \tau \leq t_{k+1}$, the linear approximation

$$\begin{aligned} V(\tau) &= V_k + \frac{V_{k+1} - V_k}{\zeta}(\tau - t_k) \\ Z(t-\tau) &= Z_{K-k} + \frac{Z_{K-(k+1)} - Z_{K-k}}{\zeta}(\tau - t_k) \end{aligned} \tag{3.3}$$

is used.

Substituting expression (3.3) into equality (3.2) and integrating with respect to τ, we obtain

$$F(K\zeta) = \sum_{n=0}^{K-1}\zeta\left\{\frac{1}{2}[V_kZ_{K-(k+1)} + V_{k+1}Z_{K-k}] + \frac{1}{3}(V_{k+1} - V_k)[Z_{K-(k+1)} - Z_{K-k}]\right\}$$

Using this representation, relations connecting the unknown quantities $\dot{q}_n(K\zeta)$ and $\ddot{a}_{jn}(K\zeta)$ can be obtained from Eq. (2.11), having differentiated it beforehand with respect to t. Substituting these relations into (2.7), we finally obtain a system of ordinary differential equations which can be written in the matrix form

$$\mathbf{B}_1^{(n)}\ddot{\mathbf{A}}_n + \mathbf{B}_2^{(n)}\mathbf{A}_n = \mathbf{C}_n$$

where the vector $\mathbf{A}_n = \{a_{0n}(K\zeta), a_{1n}(K\zeta), \ldots, a_{M,n}(K\zeta)\}^T$, $\mathbf{B}_1^{(n)}$ and $\mathbf{B}_2^{(n)}$ are square matrices, of which $\mathbf{B}_1^{(n)}$ is a completely filled matrix and $\mathbf{B}_2^{(n)}$ is a diagonal matrix, and the superscript T denotes transposition. Terms, which take account of the values of $\dot{q}_n$ and $\ddot{a}_{jn}$ in the preceding steps, occur in the vector C_n besides the right-hand side of Eq. (2.7).

4. NUMERICAL RESULTS

The results of the solution of the problem of the action of a periodic surface pressure on a circular plate floating in shallow water [1] were used to test the computational algorithm. The external pressure distribution was specified in the form (we return to dimensional variables here)

$$P(x, y, t) = a\rho g f(R)\sin\omega t$$

where

$$f(R) = \begin{cases} 1-(R/l)^2, & R<l \\ 0, & R>l \end{cases}, \quad R = \sqrt{(x-L)^2+y^2}, \quad l+L<r_0 \tag{4.1}$$

Calculations, carried out for $L = 0, r_0/2$, show that, after about 2–3 periods of $2\pi/\omega$, the oscillations of the plate reach a periodic steady state. The amplitudes of the deflections of the plate under steady conditions were identical to the results obtained previously in [1].

An external load of the form

$$P(x, y, t) = a\rho g f(R)T(t) \tag{4.2}$$

was chosen in order to investigate pulsed action on the plate.

The function $f(R)$ was given by expression (4.1) and the time dependence has the form

$$T(t) = \begin{cases} t/b, & t \le b \\ 2-t/b, & b \le t \le 2b \\ 0, & t>2b \end{cases}$$

Calculations were carried out for the following values of the initial parameters

$$D = 4.476\times10^{10}\,\text{kg m}^2/\text{s}^2, \quad H = 20\,\text{m}, \quad \rho = 10^3\,\text{kg m}^3, \quad d = 1\,\text{m},$$
$$r_0 = 200\,\text{m}, \quad l = 40\,\text{m}, \quad \nu = 0.3$$

For these values of the parameters, we have $\gamma = 5\times10^{-3}$, $\delta = 2.852\times10^{-3}$.

Calculations for a circular plate are compared with the known solution for an infinite plate (see [2, 3], for example). In the case of a load in the form of (4.2), this solution has the form

$$w(R, t) = \frac{a\rho g}{2\pi b}\int_0^\infty \frac{kY(k, t)\tilde{f}(k)J_0(kR)}{Dk^4+\rho g}dk$$

where

$$Y(k, t) = \begin{cases} \Omega^{-1}\sin\Omega t - t, & 0 \le t \le b \\ \Omega^{-1}[2\sin\Omega(b-t)+\sin\Omega t] - 2b + t, & b \le t \le 2b \\ \Omega^{-1}[2\sin\Omega(b-t)-\sin\Omega(2b-t)+\sin\Omega t], & t>2b \end{cases}$$

$$\Omega^2(k) = \frac{hk^2(Dk^4 + \rho g)}{\rho + \rho_1 h_1 hk^2}, \quad f(k) = \frac{4\pi J_2(kl)}{k^2}$$

($\tilde{f}(k)$ is the Fourier transform of the function $f(R)$ (4.41)). It was assumed that $b = 0.5$ s in the calculations presented below.

When the pressure spot is located at the centre of the plate ($L = 0$), the problem under consideration becomes axially symmetric and only the coefficients for $n = 0$ and non-zero. The transition function $G_0(\xi)$ (2.6) has the form [11]

$$G_0(\xi) = -\int_0^\infty \frac{\exp(-\xi\tau)d\tau}{\tau^2[K_1^2(\tau) + \pi^2 I_1^2(\tau)]} \tag{4.3}$$

and the approximate expression for it [13] is

$$G_0(\xi) \approx -[0.6\exp(-0.75\xi) + 0.4\exp(-0.132\xi)] \tag{4.4}$$

The time dependence of the normal deflections of the plate w/a when $r = 0$ and $r = r_0$ are shown in Fig. 1 (the solid curves in Fig. 1a and b, respectively). The time scale is given in dimensional form (the dimensionless time is obtained by normalization on the quantity $\sqrt{r_0/g} \approx 4.52$ s). For comparison, the corresponding solutions for a weightless liquid are shown in Fig. 1(a) and (b) (the dotted and dashed curves). The normal deflection of an infinite plate at the centre of application of the pressure is shown in Fig. 1(a) by dashed curve. The calculations were carried out for $M = 10$ using expression (4.3). The results for the approximation (4.4) are shown by the small open circles.

It is interesting to note that, at the centre of pressure in a time interval corresponding to the action of the pressure ($t \leqslant 2b = 1$ s), all the solutions are identical but, after the cessation of the external action, the deflections of the various plates are very different. In the case of an infinite plate, a monotonic restoration of the initial zeroth state is observed. In the case of a circular plate in a ponderable liquid, the initial state is also re-established with time but not in a monotonic manner. The maximum deflection of the edge of the plate is approximately equal to the maximum deflection at the centre of pressure and is attained when $t \approx 4.2$ s. Solutions with the exact transition function (4.3) and approximate function

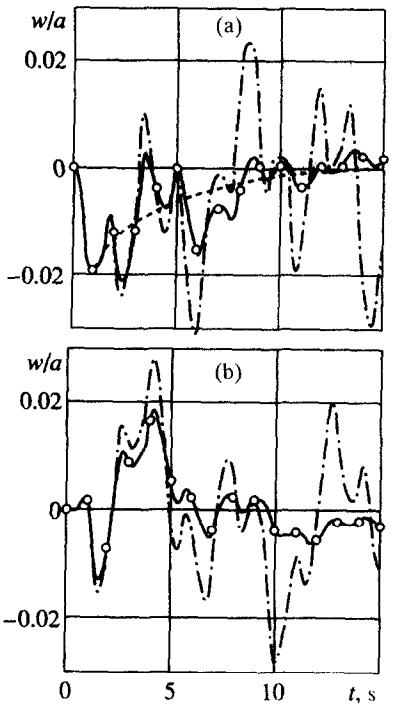

Fig. 1

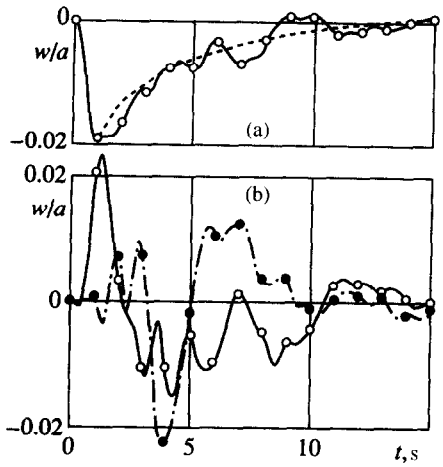

Fig. 2

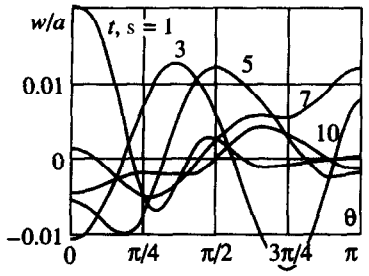

Fig. 3

transition (4.4) are practically identical and the calculations which are subsequently presented later were carried out using the approximate dependences [13] for the transition functions $G_n(\xi)$. In the case of a plate in a weightless liquid, no decrease in the deflections with time is observed either at the centre of pressure or at the edges since, in this case, there is no generation of surface waves or scattering of energy. This simpler solution can be used to obtain an upper estimate of the maximum deflections of a plate under different external actions.

The case of the asymmetric application of pressure ($L = r_0/2$) is shown in Fig. 2. The normal deflections at the centre of pressure ($x = L, y = 0$) are shown in Fig. 2(a) as a function of time for a circular plate (the solid curve) and an infinite plate (the dashed curve). As in Fig. 1(a) these solutions are identical at instants of time corresponding to the action of the pressure ($t \leq 1$ s) and then subsequently gradually tend to zero. The oscillations of the edges of the plate when $r = r_0$ are shown, for $\theta = 0$, by the solid curve in Fig. 2(b) and, when $\theta = \pi$, by the dot–dash curve in the case when $N = M = 10$. A comparison with the results of calculations when $N = M = 7$ is shown by the small open circles in Fig. 2(a) for the normal deflection at the centre of pressure and, in Fig. 2(b), for the oscillation of the edge of the plate when $\theta = 0$ and, also, by the solid points in Fig. 2(b) for the oscillation of the edge of the plate when $\theta = \pi$. It is clear that, within the above-mentioned limits, a change in the number of wave harmonics N and eigenfunctions M which are taken into account has practically no effect on the results.

The maximum values of the deflections at the left-hand and right-hand ends of a diameter passing through the centre of pressure are approximately equal and close to the values in the symmetric case (compare Fig. 1b and Fig. 2b). However, the time of the appearance of the maximum deflections is different. The fastest (at $t \approx 1.2$ s) maximum deflection of all is attained on the right-hand edge closest to the pressure domain and then at $t \approx 3.9$ s at the opposite end.

The results which have been presented confirm the conclusions [1, 7] that, in certain cases, the normal deflections of a plate on its edge exceed the corresponding values in the interior part. In this connection, it is interesting to study the behaviour of the edge of the plate in greater detail. The dependences $w(r_0\ \theta, t)$ on the angular coordinate θ at different instants of time t are shown in Fig. 3. It can be seen that, initially, the maximum deflection is attained at a point closest to the centre of pressure and the oscillations then propagate along the perimeter of the plate and are subsequently damped. A comparison

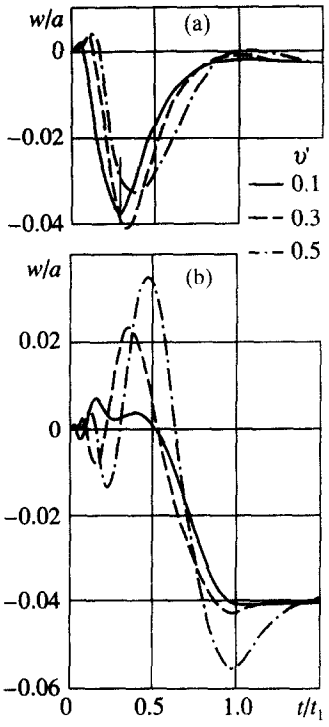

Fig. 4

of the maximum deflections on the edge and at the point $x = L, y = 0$ at the instants of time indicated (see Fig. 2a) shows that the deflections of the edge are more significant.

The effect of a moving load is demonstrated by considering an example which simulates the landing of an aircraft. It is assumed that, at the initial instant of time, the load has a speed v and smoothly touches the plate at the point $x = x_0, y = 0$ and then moves to the left in a straight line and in a uniformly decelerating manner along a diameter until it comes to a complete stop at the point $x = x_1, y = 0$ at the instant of time $t = t_1 \equiv 2(x_0 - x_1)/\upsilon$. The function on the right-hand side of Eq. (1.1) is given in the form

$$P(x, y, t) = a\rho g[1 - \exp(-bt)]f(x, y, t)$$

where the function f is defined by expression (4.1) taking into account the following time-dependence of motion of the centre of pressure

$$L(t) = \begin{cases} x_0 - \upsilon t + \dfrac{\upsilon^2 t^2}{4(x_0 - x_1)}, & 0 \le t \le t_1 \\ x_1, & t > t_1 \end{cases}$$

The previous initial parameters were used, however now $l = 0.1r_0, x_0 = 0.7r_0, x_1 = -0.7r_0, b = 20/t_1$.

The normal deflection of the plate on the axis $y = 0$ at the points $x = 0$ (a) and $x = -r_0$ (b) are shown in Fig. 4 as a function of time for different initial speeds of motion of the load $\upsilon' = \upsilon/\sqrt{gr_0}$. At the point $x = r_0, y = 0$, the maximum value of $|w/a|$ does not exceed 0.007. Note that, for the specified depth of the liquid, the dimensionless critical velocity of propagation of gravitational waves is equal to $\sqrt{H/r_0} \approx 0.33$. The instant the crest of the load intersects the origin of coordinates is shown by the vertical segment in Fig. 4(a). It can be seen that it is only in the case of relatively slow motion that the maximum deflection of the plate is attained at the instant of passage of the centre of the load. As υ' increases, the time the maximum deflection appears at the origin of coordinates is observed after the load has passed through this point. When $t > t_1$, the oscillations of the plate decay and gradually take values corresponding to a distributed static load centred at the point $x = x_1, y = 0$. The solution of this steady problem is easily constructed using the method described above, where the system of ordinary differential equations (2.7)

reduces to a simple system of linear algebraic equations. The dimensionless values of the static deflection on the axis $y = 0$ when $x = 0$ and $x = -r_0$ are equal to –0.002 and –0.041 respectively. The results shown in Fig. 4 were obtained for $N = M = 7$.

Note that the method proposed can be extended to investigating the transient hydroelastic behaviour of a circular plate floating on the surface of a liquid of finite and infinite depth.

I wish to thank A. A. Korobkin for useful discussions and remarks.

This research was supported financially by the Russian Foundation for Basic Research (02-01-00739) the "State Support of Leading Scientific Schools" Programme (00-15-96162) and the Integrated Project No. 1 of the Siberian Branch of the Russian Academy of Sciences.

REFERENCES

1. STUROVA, I. V., The action of periodic surface pressures on a floating elastic platform. *Prikl. Mat. Mekh.*, 2002, **66**, 1, 75–86.
2. HEISIN, D. E., *Dynamics of an Ice Sheet*, Gidrometeoizdat, Leningrad, 1967.
3. CHERKESOV, L. V., *Surface and Internal Waves*, Naukova Dumka, Kiev, 1973.
4. SQUIRE, V. A., HOSKING, R. J., KERR A. D. and LANGHORNE, P. J., *Moving Loads on Ice Plates*. Kluwer, Dordrecht, 1996.
5. OHMATSU, S., Numerical calculation of hydroelastic behaviour of VLFS in time domain. *Hydroelasticity in Marine Technology: Proc. 2nd Intern. Conf. Fukuoka*: Res. Inst. Appl. Mech., Kyushu Univ., 1998, 89–97.
6. KASHIWAGI, M., A time-domain mode-expansion method for calculating transient elastic responses of a pontoon-type VLFS. *J. Mar. Sci. Technol.*, 2000, **5**, 89–100.
7. STUROVA, I. V., The unsteady behaviour of an elastic beam floating in shallow water under the action of an external load. *Zh. Prikl. Mekh. Tekh. Fiz.*, 2002, **43**, 3, 88–98.
8. KOROBKIN A., Unsteady hydroelasticity of floating plates. *J. Fluids Struct.*, 2000, **14**, 971–991.
9. GONTKEVICH, V. S., *Natural Oscillations of Plates and Shells, A Handbook*, Naukova Dumka, Kiev, 1964.
10. ITAO, K., Crandall, S. H., Natural modes and natural frequencies of uniform, circular, free-edge plates. *Trans. ASME. J. Appl. Mech.*, 1979, **46**, 448–453,
11. GRIGOLYUK, E. I. and GORSHKOV, A. G., *The Unsteady Hydroelasticity of Shells*, Sudostroyeniye, Leningrad, 1974.
12. RANDALL, D. C., Supersonic flow past quasi-cylindrical bodies of almost circular cross-section. *Aeronauf. Res. Council, Rep. Mem.*, 1958, **3067**.
13. LECLERC, J., Étude du flottement des coques cylindriques minces dans le cadre de la théorie du potentiel linearisé, 1. Détermination des forces aérodynamiques. *J. méc.*, 1970, **9**, 111–154.

Translated by E.L.S.